International Journal of Minerals, Metallurgy and Materials
Volume 24, Number 3, March 2017, Page 289
DOI: 10.1007/s12613-017-1407-4

Oxidation and interdiffusion behavior of a germanium-modified silicide coating on an Nb–Si-based alloy

Jin-long Li, Wan Wang, and Chun-gen Zhou

Department of Materials Science and Engineering, Beihang University, Beijing 100191, China
(Received: 4 August 2016; revised: 3 November 2016; accepted: 7 November 2016)

Abstract: To investigate the interdiffusion behavior of Ge-modified silicide coatings on an Nb–Si-based alloy substrate, the coating was oxidized at 1250°C for 5, 10, 20, 50, or 100 h. The interfacial diffusion between the $(Nb,X)(Si,Ge)_2$ (X = Ti, Cr, Hf) coating and the Nb–Si based alloy was also examined. The transitional layer is composed of $(Ti,Nb)_5(Si,Ge)_4$ and a small amount of $(Nb,X)_5(Si,Ge)_3$. With increasing oxidation time, the thickness of the transitional layer increases because of the diffusion of Si from the outer layer to the substrate, which obeys a parabolic rate law. The parabolic growth rate constant of the transitional layer under oxidation conditions is 2.018 $\mu m \cdot h^{-1/2}$. Moreover, the interdiffusion coefficients of Si in the transitional layer were determined from the interdiffusion fluxes calculated directly from experimental concentration profiles.

Keywords: silicides; coatings; intermetallics; oxidation; interdiffusion

1. Introduction

In the next-generation jet engines, the maximum service temperature will increase from 1150°C to 1300°C, which would cause nickel-based superalloys to enter a liquid-phase state, prompting research into new alloy systems [1–8]. Therefore, there has been considerable interest in developing structural materials that can withstand severe environments at elevated temperatures. Nb–Si-based *in situ* composites with a microstructure consisting of niobium solid solution (Nb_{ss}) and Nb_5Si_3 phases exhibit excellent potential as high-temperature-resistant materials because of their low density, high strength, and high melting points at elevated temperatures [9–10]. However, a major barrier to the high-temperature applications of Nb–Si-based alloys is their poor oxidation resistance. Elements such as Cr, Al, Hf, Sn, and B [11–13] have been used as modifiers to improve the high-temperature oxidation resistance of Nb–Si-based *in situ* composites; however, few satisfactory results have been reported.

Depositional coatings offer a promising approach to improve the long-term environmental stability of Nb–Si-based alloys at high temperatures [14–15]. An $NbSi_2$ coating formed on the surface is the most promising candidate material resulting from the formation of SiO_2. However, the oxidation resistance of single binary disilicide ($NbSi_2$) is limited because the scale formed after oxidation contains visible cracks and numerous pores, which would readily lead to the emergence of wrinkling and breakdowns [16]. To overcome this limitation, a large number of studies have been conducted using the pack cementation process to develop the silicide coatings modified with elements such as Al, B, Ge, and Cr [17–22]. The addition of Ge, in particular, has been demonstrated to be a useful modifying element to improve the oxidation resistance of the silicide coatings in our previous studies [20,23].

Ge-modified silicide coatings can efficiently prevent the substrate from being oxidized by forming glassy SiO_2 and GeO_2. The GeO_2 decreases the adhesiveness of SiO_2 glass at high temperatures, which results in a better sealant and substantially increases the expansion coefficient [24–25]. However, data related to the diffusion characteristics of such coatings are insufficient and the basic aspects of the diffusion properties of silicides are still scarcely known. Ex-

Corresponding author: Chun-gen Zhou E-mail: cgzhou@buaa.edu.cn

panding the applications of Ge-modified silicide coatings requires reliable data concerning the solid-state interdiffusion properties of silicides at high temperatures. Therefore, the objective of the present work is to investigate the interdiffusion behavior of the Ge-modified silicide coatings on Nb–Si-based alloys under oxidation conditions at high temperatures.

2. Experimental

2.1. Specimen preparation

The Nb–Si-based alloy with a nominal composition of Nb–16Si–22Ti–17Cr–2Al–2Hf (at%) prepared by vacuum non-consumable arc-melting under an argon atmosphere was used as a substrate material for the coating experiments. To ensure composition homogeneity and element partitioning, a remelting treatment was applied more than five times. The microstructure of the arc-melted alloy was composed of primary large $(Nb,X)_5Si_3$ (X = Ti, Cr, Hf) blocks, Nb solid solution (Nb_{ss}), and Cr_2Nb [26]. Before the coating experiments, the alloy ingot was machined into slices approximately 8 mm in diameter and 3 mm in thickness, and all six sides of each specimen were ground to an 800-grit level with sandpapers. The samples were then ultrasonically cleaned in acetone and finally dried.

2.2. Coating process

Pure Si and Ge powders were used as donor sources, and NaF and Al_2O_3 powders were used as the activator and filler in the pack mixture, respectively. After the components were weighed, mixed, and ground, the pack with a chemical composition of 16Si–8Ge–5NaF–71Al_2O_3 (wt%) was used to co-deposit Si and Ge; the composition was obtained by reference to our previous paper [20]. We prepared the packs by burying the substrates in a well-mixed pack powder mixture in an alumina crucible. The crucibles were then heated at 1300°C for 10 h, and the furnace was then cooled to room temperature naturally by switching off the power supply.

2.3. Oxidation test

The oxidation tests were conducted in an open-ended tube electric furnace at 1250°C isothermally. High-purity alumina crucibles were used to support the specimens during the oxidation experiments. The hot zone of the electrical furnace was maintained for 5, 10, 20, 50, and 100 h, respectively, after which the specimens were removed to cool at room temperature.

2.4. Analyzing methods

X-ray diffraction (XRD, model D/Max 2500PC, Rigaku, Japan) using Cu K_α radiation was used to identify the phases present in the specimens. The microstructure and the chemical compositions of the constituent phases were analyzed either by scanning electron microscopy (FESEM, JSM-7500F, Japan) on an instrument equipped for energy-dispersive X-ray spectroscopy (EDS, Inca X-sight) or by electron-probe microanalysis (EPMA, model JXA-8230, Japan) with wavelength-dispersive spectroscopy (WDS).

3. Results and discussion

3.1. Microstructure of as-deposited coatings

Fig. 1(a) shows a typical cross-sectional BSE image of the Ge-modified silicide coating prepared by co-depositing Si and Ge at 1300°C for 10 h. A uniform coating with a thickness of approximately 160 μm formed on the Nb–Si alloy. The coating is relatively dense and metallurgically

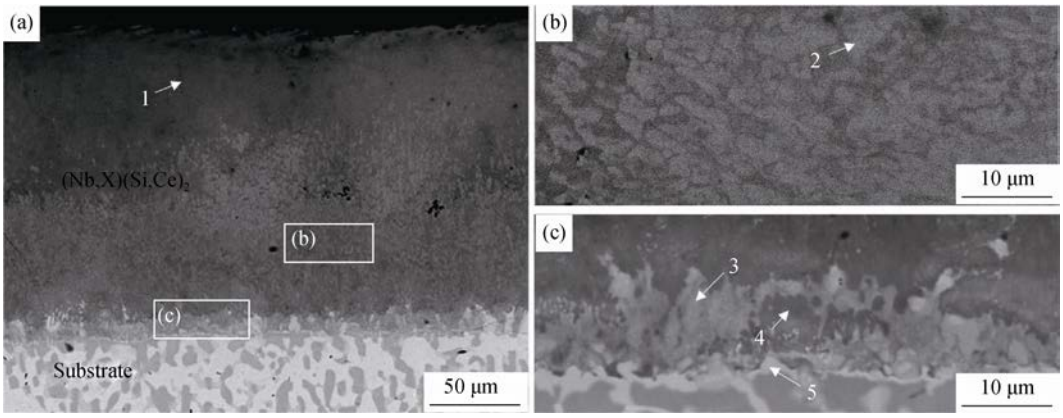

Fig. 1. (a) BSE image of the Ge-modified silicide coating prepared by co-depositing Si and Ge at 1300°C for 10 h; (b) enlarged BSE image of the coating (indicated by a rectangular window (b) in figure (a)); (c) enlarged BSE image of the interface zone between the transitional layer and the substrate (indicated by a rectangular window (c) in figure (a)).

bonded to the substrate. The structure of the coating is divided into an outer layer and a transitional layer underneath.

As shown in Fig. 1(a), the outer layer consists of a gray matrix with some bright particles located in its lower portion. WDS analysis demonstrates that the gray matrix (Fig. 1(a), point 1) has a typical composition of 65.7Si–9.8Ti–7.5Cr–1.7Ge–14.8Nb–0.5Hf (at%) and that the bright particles (Fig. 1(b), point 2) have a typical composition of 58.5Si–10.3Ti–8.7Cr–2.5Ge–18.5Nb–1.5Hf (at%), confirming that both the gray matrix and the bright particles in the outer layer are $(Nb,X)(Si,Ge)_2$. We obtained similar results in a previous study [20]. The bright particles are rich in Hf and Ti but are slightly deficient in Si compared to the stoichiometric $NbSi_2$. According to the original microstructure and composition of the substrate alloy [27], the primary $(Nb,X)_5Si_3$ rich in Ti and Hf elements exists in the form of big blocks. Considering that the formation of the $(Nb,X)(Si,Ge)_2$ layer is dominated by the inward diffusion of Si, we deduced that some embedded primary $(Nb,X)_5Si_3$ particles from the substrate are transformed into $(Nb,X)(Si,Ge)_2$ particles with higher Ti and Hf contents, as has been discussed by Guo *et al.* [28].

As shown in Fig. 1(c), a transitional layer with a thickness of approximately 14 μm is formed between the coating and the substrate. The transitional layer is composed of light-gray blocks (point 3) and a gray matrix (point 4). The WDS analysis results indicate that the composition of the light-gray blocks is 45.1Si–10.8Ti–0.7Cr–1.5Ge–40.1Nb–1.8Hf (at%) and that the composition of the gray matrix is 44.7Si–14.3Ti–12.6Cr–1.7Ge–25.9Nb–0.8Hf (at%). On the basis of the WDS analysis results and the XRD pattern (collected on the surface after the coating being stripped off 150 μm) (Fig. 2), both light-gray blocks and a gray matrix in the transitional layer were identified as $(Ti,Nb)_5(Si,Ge)_4$. In addition, the gray matrix is rich in Cr compared to the corresponding light-gray blocks. Moreover, a small amount of phases (point 5) are formed underneath the $(Ti,Nb)_5(Si,Ge)_4$. On the basis of the ternary Nb–Si phase diagram [29–30] and EDS analysis results, the phase with the composition of 36.1Si–15Ti–8Cr–1.1Ge–38.2Nb–1.6Hf (at%) is presumed to be $(Nb,X)_5(Si,Ge)_3$, which is consistent with the results reported in the literature [31].

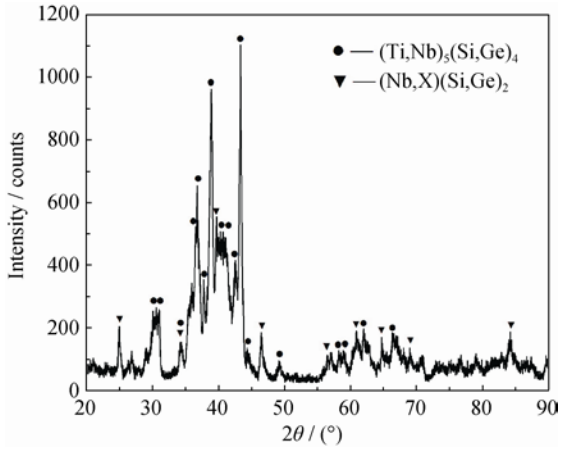

Fig. 2. XRD pattern of the surface after the 150 μm Ge-modified silicide coating was stripped from the substrate.

3.2. Microstructure evolution of the coatings

Fig. 3 presents the cross-sectional BSE images of the Ge-modified silicide coatings exposed to air at 1250°C for 5, 10, 20, 50, and 100 h. The coatings oxidized for different times exhibit similar structures that mainly consist of a thick outer layer and a thin transitional layer. As shown in Figs. 3(a–e), a continuous and compact oxide scale is formed on the surface of the sample. The thickness of oxide scale increases from 9 to 36 μm when the oxidation time increases from 5 to 100 h. The thickness of the transitional layer continues to increase substantially with increasing oxidation time. The main reasons for the thickness change of the coating layers might be the inward diffusion of Si and the interdiffusion between the coating and the substrate with increasing holding time [32]. Moreover, more micropores appear in the $(Nb,X)(Si,Ge)_2$ layer with increasing oxidation time, which might be caused by the Kirkendall effect.

To understand the effect of interdiffusion on the microstructure evolution in the aforementioned samples, we plotted the Si, Ge, Ti, Nb, Cr, and Hf concentrations at the position approximately 10 μm from the coating surface after the Ge-modified silicide coatings were oxidized at 1250°C for various times (Fig. 4). As evident in Fig. 4, the concentration of Si in the outer layer decreases and that of Nb tends to increase with increasing oxidation time. These results indicate that the coating is formed predominantly through inward diffusion of Si. Meanwhile, the inward diffusion of Si from the coating to the substrate increases the ratio of Nb in the outer layer. In addition, the concentrations of Ti and Cr slightly decrease; this observation is attributed to the formation of TiO_2 and Cr_2O_3 [20]. The concentrations of Ge and Hf nearly keep at a constant when the oxidation time increases from 5 to 100 h. The interdiffusion behavior between the coating and the substrate may change the original chemical composition of the coating, thus resulting in diminished high-temperature oxidation resistance.

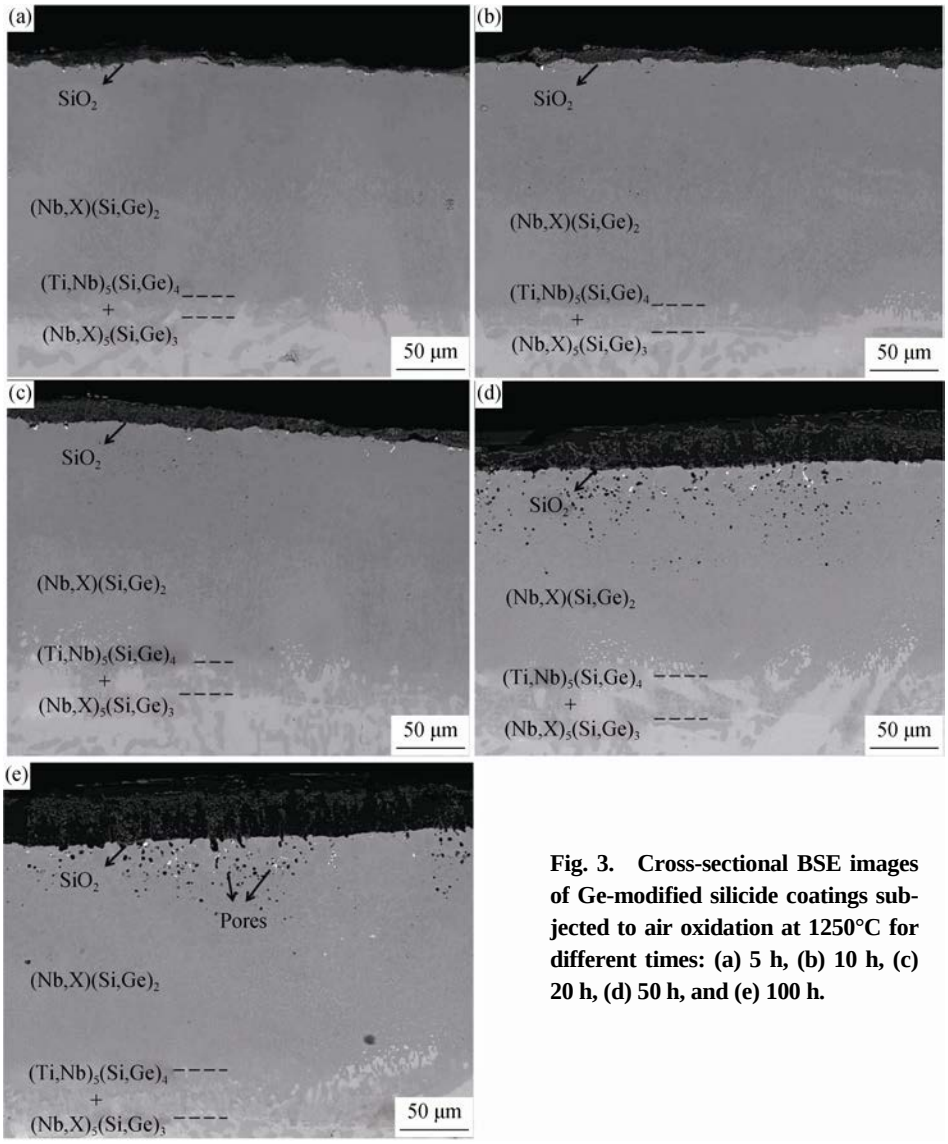

Fig. 3. Cross-sectional BSE images of Ge-modified silicide coatings subjected to air oxidation at 1250°C for different times: (a) 5 h, (b) 10 h, (c) 20 h, (d) 50 h, and (e) 100 h.

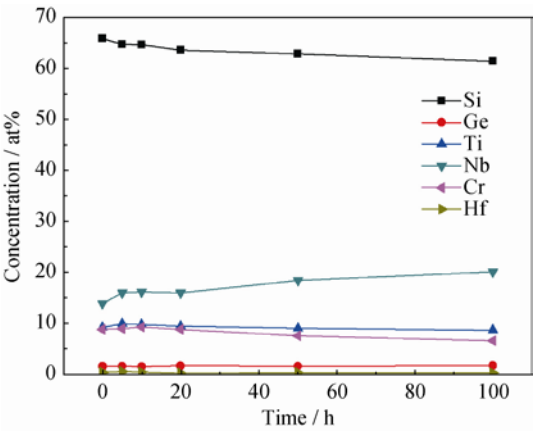

Fig. 4. Element concentration profiles at the position approximately 10 μm from the surface of the Si–Ge coatings oxidized at 1250°C for 5–100 h.

3.3. Growth behavior of transitional layer

According to our previous studies [20,23], the formation of the coating is dominated by the inward diffusion of Si and Ge. At the initial stage of the deposition process, Si and Ge diffuse to the surface of the substrate. $(Nb,X)_5(Si,Ge)_3$ can be initially formed in the substrate by reaction (1). With the inward movement of the Si, the $(Nb,X)_5(Si,Ge)_3$ phase is converted into the $(Ti,Nb)_5(Si,Ge)_4$ phase, as shown in reaction (2). As a result, the transitional layer containing the $(Nb,X)_5(Si,Ge)_3$ phase and the $(Ti,Nb)_5(Si,Ge)_4$ phase is formed in the substrate.

$$5(Nb,X) + 3([Si],[Ge]) \rightarrow (Nb,X)_5(Si,Ge)_3 \quad (1)$$

$$(Nb,X)_5(Si,Ge)_3 + [Si] \rightarrow (Ti,Nb)_5(Si,Ge)_4 \quad (2)$$

As shown in reaction (3), with increasing holding time,

inwardly diffused [Si] further reacts with $(Ti,Nb)_5(Si,Ge)_4$, resulting in the formation of the $(Nb,X)(Si,Ge)_2$ phase, which leads to the formation of the outer layer. A similar analysis has been reported elsewhere by Zhang *et al.* [22].

$$(Ti,Nb)_5(Si,Ge)_4 + [Si] \rightarrow (Nb,X)(Si,Ge)_2 \quad (3)$$

As evident in Fig. 3, the transitional layer becomes thicker with increasing oxidation time. The growth mechanism of the transitional layer can be analyzed with respect to the diffusion of components. As is well known, the concentration of Si in the $(Nb,X)(Si,Ge)_2$ layer is higher than that in the transitional layer, which is composed of $(Ti,Nb)_5(Si,Ge)_4$ and a small amount of $(Nb,X)_5(Si,Ge)_3$. The Si atoms will diffuse from the coating to the substrate because of the concentration gradient. In addition, some experiments have been carried out to demonstrate that the diffusion of Si is much faster than that of Nb [33–34]. Therefore, the inward diffusion of Si plays a key role in increasing the thickness. With an increase in the oxidation time, the growth of the $(Nb,X)_5(Si,Ge)_3$ phase is a result of the reaction of inward [Si] and [Ge] with (Nb,X) in the substrate via Eq. (1). Because of the persistent inward diffusion of Si from the outer layer, the resultant $(Nb,X)_5(Si,Ge)_3$ immediately reacts with [Si] to form $(Ti,Nb)_5(Si,Ge)_4$, as shown in Eq. (2). Meanwhile, as the amount of Si decreases in the outer layer, the $(Nb,X)(Si,Ge)_2$ layer degrades into an $(Ti,Nb)_5(Si,Ge)_4$ layer. Consequently, the $(Ti,Nb)_5(Si,Ge)_4$ transitional layer grows beneath the $(Nb,X)(Si,Ge)_2$ layer.

The thickness of the $(Nb,X)(Si,Ge)_2$ layer and the oxidation resistance of the coating are influenced by the growth rate of the diffusion layer. When the $(Nb,X)(Si,Ge)_2$ phase completely changes into the transitional phase, the coating is only protected by the outer SiO_2 layer. Any damage, such as spalling or crack formation, will lead to serious oxidation of the coating and the Nb–Si-based alloy substrate. Therefore, investigating the growth kinetics of the transitional layer is important.

Fig. 5(a) illustrates the growth kinetics of the transitional layer system under oxidation conditions. The coating thickness is taken at an average value from 10 measured places for each coated specimen. The thickness of the transitional layer at oxidation time = 0 corresponds to that of the layer formed during the pack cementation. The layer growth kinetics conforms well to the parabolic rate law. We observed that, with increasing oxidation time, the thickness of the transitional layer continues to increase. The diffusion of Si through the transitional layer is the rate-determining step in the growth of the transitional layer.

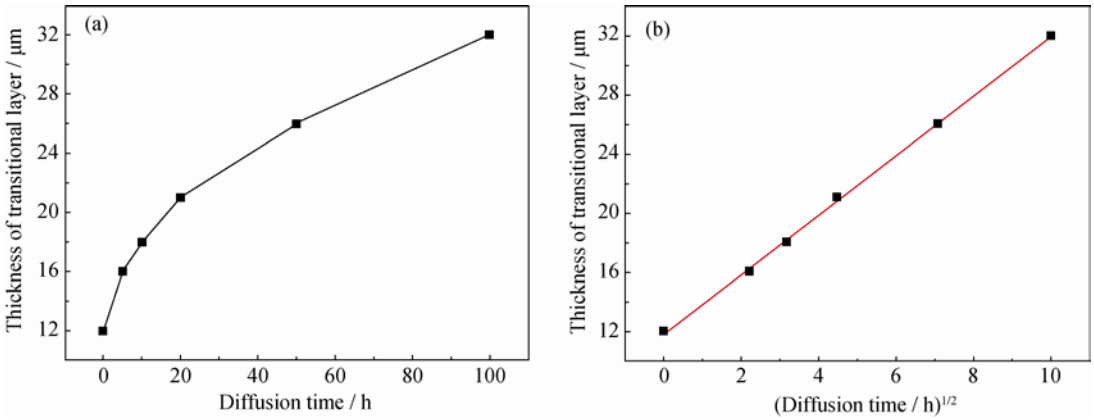

Fig. 5. (a) Thickness of the transitional layer as a function of oxidation time and (b) relation between the thickness of the transitional layer and the square root of the oxidation time.

As shown in Fig. 5(b), a linear relationship is obtained when the thickness of the transitional layer is plotted against the square root of time. The growth kinetics of the transitional layer obeys a parabolic rate law, as shown in Eq. (4):

$$d = k\,t^{1/2} + b \quad (4)$$

where d, k, t, and b are the thickness of the transitional layer, the parabolic rate constant, the oxidation time, and the offset value, respectively.

The solid straight line in Fig. 5(b) is the least-squares fit to the data points, which gives

$$d = 2.018\,t^{1/2} + 11.774 \quad (5)$$

Thus, the parabolic rate constant is relatively low for the growth rate of the transitional layer under oxidation conditions [26], which could guarantee the better oxidation resistance of $(Nb,X)(Si,Ge)_2$ coating on the Nb–Si-based alloys.

3.4. Interdiffusion flux and interdiffusion coefficient

To further understand the diffusion of Si in the coating, we investigated the concentration profiles of Si across the thickness of the oxidized samples by EPMA to characterize the distribution of the Si. Figs. 6(a) and 6(b) present the

coatings oxidized at 1250°C for 20 h and 100 h. Because the concentrations of the $(Nb,X)_5(Si,Ge)_3$ phase and the Ge atoms in the transitional layer are extremely low, they were ignored in this study. Before the determination of interdiffusion fluxes of Si, the experimental concentration profiles were first smoothed using a series of weighted splines. Moreover, the error of the smooth was restricted to below 5%, which is acceptable for the following calculation. The interdiffusion flux of Si can be obtained at any section x directly from the concentration profiles using the method developed by Dayananda [35]. The relative concentration variable Y is introduced and defined as a function of distance x over the diffusion zone between L^- and L^+:

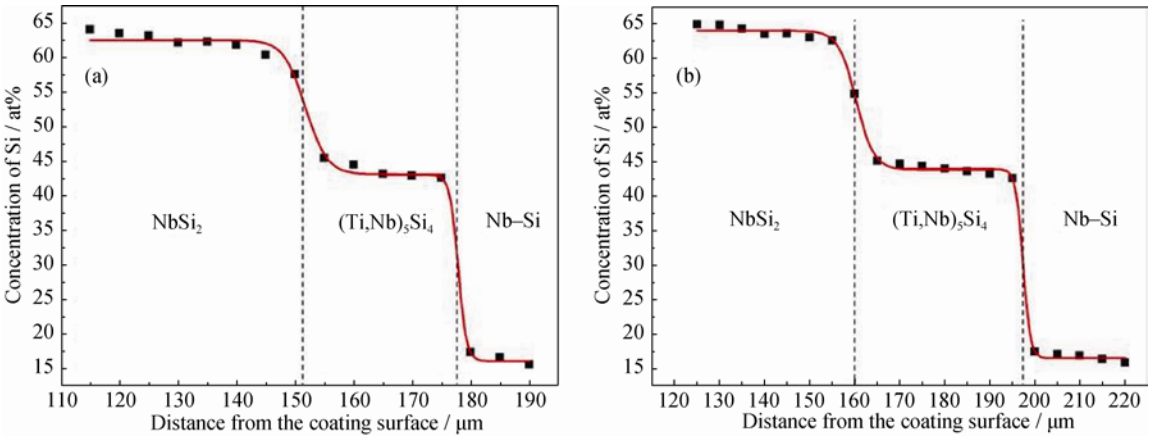

Fig. 6. EPMA composition profiles of Si in the coatings oxidized at 1250°C for (a) 20 h and (b) 100 h.

$$Y = \frac{C - C^+}{C^- - C^+} \tag{6}$$

where C refers to the initial concentration of Si as a function of distance x. C^- and C^+ are the initial concentrations at $x = L^-$ and $x = L^+$, respectively. In the theory of Dayananda [35], the following equation is also deduced:

$$\int_{L^-}^{x}(1-Y)\mathrm{d}x - \int_{x}^{L^+} Y\mathrm{d}x = x - x_0 \tag{7}$$

On the basis of Eqs. (6) and (7), the interdiffusion flux $\tilde{J}$ of Si at any section x^* in the diffusion zone between an $NbSi_2$ coating and Ni–Si is given by

$$\tilde{J}(x^*) = \frac{C^- - C^+}{2t}\left[Y^*\int_{L^-}^{x^*}(1-Y)\mathrm{d}x + (1-Y^*)\int_{x^*}^{L^+} Y\mathrm{d}x\right] \tag{8}$$

where t is the time of diffusion. In addition, x_0 denotes the position of the so-called Matano plane, defined by Eq. (9):

$$x_0 = L^- + \int_{L^-}^{L^+} Y\mathrm{d}x \tag{9}$$

Using the concentration profiles data for the coating oxidized at 1250°C for 20 h and 100 h, we obtained values of $\tilde{J}$ using Eq. (8) for Si as a function of the distance x from the coating surface; the results are shown in Fig. 7. The interdiffusion flux of Si obtained at 20 h is 1.9×10^{-9} at%·cm·s^{-1}, which is greater than 6.0×10^{-10} at%· cm·s^{-1} at 100 h in the transitional layer. These results indicate the diffusion of Si from the outer layer to the substrate becomes slower with the oxidation time increasing from 20 h to 100 h. According to the growth mechanism of the above transitional layer, we concluded that the growth rate of the transitional layer decreases with increasing oxidation time. This behavior explains why the transitional layer growth kinetics conforms to a parabolic rate law.

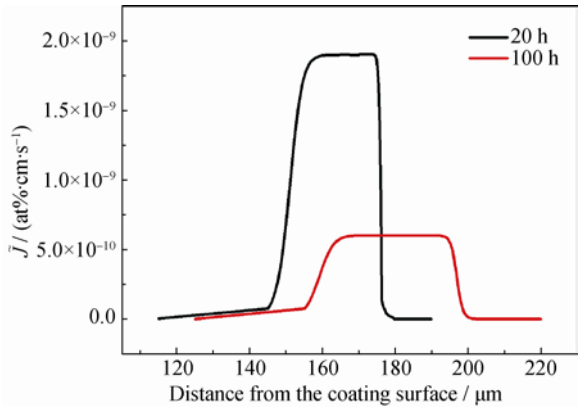

Fig. 7. Interdiffusion fluxes of Si in the transitional layer after the coating was oxidized at 1250°C for 20 h and 100 h.

For $(Ti,Nb)_5Si_4$ phase with a very narrow range of homogeneity—the so-called "line compounds", it is difficult to obtain the concentration dependence interdiffusion coefficients of Si for . According to the theory of Tortorici and Dayananda [36], the integrated and average effective interdiffusion coefficients are readily available and accurate for describing the diffusion behavior. Over a concentration range from $C(x_1)$ to $C(x_2)$ in the transitional layer, an inte-

grated interdiffusion coefficient, $\tilde{D}_{\text{int}}$, is defined by

$$\tilde{D}_{\text{int}} = \int_{x_1}^{x_2} \tilde{J} \mathrm{d}x \tag{10}$$

In addition, the average effective interdiffusion coefficient, $\tilde{D}_{\text{eff}}$, of Si over the concentration range is also defined by

$$\tilde{D}_{\text{eff}} = \frac{\tilde{D}_{\text{int}}}{C(x_1) - C(x_2)} \tag{11}$$

From profiles of concentration (Fig. 6) and interdiffusion fluxes (Fig. 7) in $NbSi_2$/Nb–Si diffusion couples, the integrated and average effective interdiffusion coefficients for the line compound, i.e., $(Ti,Nb)_5Si_4$, are calculated by Eqs. (10) and (11), respectively. The integrated interdiffusion coefficient of Si in the transitional layer oxidized at 1250°C for 20 h is 4.77×10^{-12} cm^2/s, whereas for 100 h, the integrated interdiffusion coefficient of Si is 2.28×10^{-12} cm^2/s. On the basis of Eq. (11), to calculate the average effective interdiffusion coefficients for $(Ti,Nb)_5Si_4$, the homogeneity ranges for this phase must be achieved. According to Yeh *et al.* [37], the Si concentration difference of Ti_5Si_4 is 5.5at%. As a result, the average effective interdiffusion coefficients of Si for 20 and 100 h are 8.67×10^{-11} cm^2/s and 4.15×10^{-11} cm^2/s, respectively. It can be seen that the values of the integrated and average effective interdiffusion coefficients of Si show the decreasing trend with the rise of the oxidation time.

In conclusion, these sets of interdiffusion data lay a foundation for understanding the diffusion processes of Si in Ge-modified silicide coatings on Nb–Si-based alloy.

4. Conclusions

(1) Ge-modified silicide coating on the niobium silicides substrate was successfully prepared. The coating consists of a thick $(Nb,X)(Si,Ge)_2$ (X = Ti, Cr, Hf) outer layer and a thin transitional layer composed of $(Ti,Nb)_5(Si,Ge)_4$ phase and a small amount of $(Nb,X)_5(Si,Ge)_3$ phase.

(2) The growth of the transitional layer is dominated by the diffusion of Si from the coating to the substrate and obeys a parabolic rate law. The parabolic growth rate constant of the transitional layer under oxidation condition at 1250°C is 2.018 $\mu m \cdot h^{-1/2}$. Moreover, the integrated and average interdiffusion coefficients of Si are determined from the interdiffusion fluxes, which are calculated directly from experimental concentration profiles for 20 and 100 h.

Acknowledgements

This work is financially supported by the National Natural Science Foundation of China (No. 51431003) and the Joint Funds of the National Natural Science Foundation of China (No. U1435201).

References

[1] J.H. Perepezko, The hotter the engine, the better, *Science*, 326(2009), No. 5956, p. 1068.

[2] W.Y. Gong, L.J. Zhang, D.Z. Yao, and C.G. Zhou, Diffusivities and atomic mobilities in fcc Ni–Pt alloys, *Scripta Mater.*, 61(2009), No. 1, p. 100.

[3] C.G. Zhou, C.L. Wang, and Y.X. Song, Evaluation of cyclic oxidation of thermal barrier coatings exposed to NaCl vapor by finite element method, *Mater. Sci. Eng. A*, 490(2008), No.1-2, p. 351.

[4] K.M. Emran, S.T. Arab, A.M. Al-Turkustani, and H.A. Al-Turaif, Temperature effect on the corrosion and passivation characterization of $Ni_{82.3}Cr_7Fe_3Si_{4.5}B_{3.2}$ alloy in acidic media, *Int. J. Miner. Metall. Mater.*, 23(2016), No. 2, p. 205.

[5] C.G. Zhou, J.S. Yu, S.K. Gong, and H.B. Xu, Influence of water vapor on the high temperature oxidation behavior of thermal barrier coatings, *Mater. Sci. Eng. A*, 348(2003), No. 1-2, p. 327.

[6] H.B. Guo, S.K. Gong, C.G. Zhou, and H.B. Xu, Investigation on hot-fatigue behaviors of gradient thermal barrier coatings by EB-PVD, *Surf. Coat. Technol.*, 148(2001), No. 2-3, p. 110.

[7] U.P. Kumar and C.J. Kennady, Effect of benzaldehyde on the electrodeposition and corrosion properties of Ni–W alloys, *Int. J. Miner. Metall. Mater.*, 22(2015), No. 10, p. 1060.

[8] H. Huang, C. Liu, L.Y. Ni, and C.G. Zhou, Evaluation of microstructural evolution of thermal barrier coatings exposed to Na_2SO_4 using impedance spectroscopy, *Corros. Sci.*, 53(2011), No. 4, p. 1369.

[9] D.Z. Yao, R. Cai, C.G. Zhou, J.B. Sha, and H.R. Jiang, Experimental study and modeling of high temperature oxidation of Nb-base *in situ* composites, *Corros. Sci.*, 51(2009), No. 2, p. 364.

[10] Z. Yazdani, F. Karimzadeh, M.H. Abbasi, and A. Amini, Characterization of $NbSi_2$–Al_2O_3 nanocomposite coatings prepared with plasma spraying mechanically alloyed powders, *Int. J. Miner. Metall. Mater.*, 22(2015), No. 7, p. 748.

[11] K. Zelenitsas and P. Tsakiropoulos, Effect of Al, Cr and Ta additions on the oxidation behaviour of Nb–Ti–Si *in situ* composites at 800°C, *Mater. Sci. Eng. A*, 416(2006), No. 1-2, p. 269.

[12] J. Wang, X.P. Guo, and J.M. Guo, Effects of B on the microstructure and oxidation resistance of Nb–Ti–Si-based ultra-high-temperature alloy, *Chin. J. Aeronaut*, 22(2009), No. 5, p. 544.

[13] J. Geng and P. Tsakiropoulos, A study of the microstructures and oxidation of Nb–Si–Cr–Al–Mo *in situ* composites alloyed with Ti, Hf, Sn, *Intermetallics*, 15(2007), No. 3, p. 382.

[14] A. Rauf, Q. Yu, L. Jin, and C. Zhou, Microstructure and thermal properties of nanostructured lanthana-doped yttria-stabilized zirconia thermal barrier coatings by air plasma spraying, *Scripta Mater.*, 66(2012), No. 2, p. 109.

[15] S. Majumdar, A. Arya, I.G. Sharma, A.K. Suri, and S. Banerjee, Deposition of aluminide and silicide based protective coatings on niobium, *Appl. Surf. Sci.*, 257(2010), No. 2, p. 635.

[16] T.P. Chow, K. Hamzeh, and A.J. Steckl, Thermal oxidation of niobium silicide thin films, *J. Appl. Phys.*, 54(1983), No. 5, p. 2716.

[17] X.D. Tian and X.P. Guo, Structure of Al-modified silicide coatings on an Nb-based ultrahigh temperature alloy prepared by pack cementation techniques, *Surf. Coat. Technol.*, 203(2009), No. 9, p. 1161.

[18] A.E. Kudryashov, A.Y. Potanin, D.N. Lebedev, I.V. Sukhorukova, D.V. Shtansky, and E.A. Levashov, Structure and properties of Cr–Al–Si–B coatings produced by pulsed electrospark deposition on a nickel alloy, *Surf. Coat. Technol.*, 285(2016), p. 278.

[19] Y.Q. Qiao and X.P. Guo, Formation of Cr-modified silicide coatings on a Ti–Nb–Si based ultrahigh-temperature alloy by pack cementation process, *Appl. Surf. Sci.*, 256(2010), No. 24, p. 7462.

[20] W. Wang, B.F. Yuan, and C.G. Zhou, Formation and oxidation resistance of germanium modified silicide coating on Nb based *in situ* composites, *Corros. Sci.*, 80(2014), p. 164.

[21] J. Pang, W. Wang, and C.G. Zhou, Microstructure evolution and oxidation behavior of B modified $MoSi_2$ coating on Nb-Si based alloys, *Corros. Sci.*, 105(2016), p. 1.

[22] Z.K. Zheng, W.M. Mao, Z.Y. Liu, D. Wang, and R. Yue, Refinement of primary Si grains in Al–20% Si alloy slurry through serpentine channel pouring process, *Int. J. Miner. Metall. Mater.*, 23(2016), No. 5, p. 572.

[23] W. Wang and C.G. Zhou, Characterization of microstructure and oxidation resistance of Y and Ge modified silicide coating on Nb–Si based alloy, *Corros. Sci.*, 110(2016), p. 114.

[24] A. Mueller, G. Wang, and R.A. Rapp, Oxidation behavior of tungsten and germanium-alloyed molybdenum disilicide coatings, *Mater. Sci. Eng. A*, 155(1992), No. 1-2, p. 199.

[25] B.V. Cockeram and R.A. Rapp, Oxidation-resistant boron- and germanium-doped silicide coatings for refractory metals at high temperature, *Mater. Sci. Eng. A*, 192-193(1995), p. 980.

[26] P. Zhang and X.P. Guo, Y and Al modified silicide coatings on an Nb-Ti-Si based ultrahigh temperature alloy prepared by pack cementation process, *Surf. Coat. Technol.*, 206(2011), No. 2-3, p. 446.

[27] W. Wang and C.G. Zhou, Hot corrosion behaviour of $Nbss/Nb_5Si_3$ *in situ* composites in the mixture of Na_2SO_4 and NaCl melts, *Corros. Sci.*, 74(2013), p. 345.

[28] Z.P. Sun, X.P. Guo, and B.H. Guo, Effect of B and Ti on the directionally solidified microstructure of the Nb–Si alloys, *Int. J. Refract. Met. Hard Mater.*, 51(2015), p. 243.

[29] J.C. Zhao, M.R. Jackson, and L.A. Peluso, Determination of the Nb–Cr–Si phase diagram using diffusion multiples, *Acta Mater.*, 51(2003), No. 20, p. 6395.

[30] G. Shao, Thermodynamic modelling of the Cr–Nb–Si system, *Intermetallics*, 13(2005), No. 1, p. 69.

[31] X. Li, X.P. Guo, and Y.Q. Qiao, Structure and oxidation behavior of Zr–Y modified silicide coatings prepared on an Nb–Ti–Si–Cr based ultrahigh temperature alloy, *Oxid. Met.*, 83(2015), No. 3, p. 253.

[32] F. Michihisa, M. Yuzi, H. Shigenari, N. Toshio, S. Kazusi, K. Akio and T. Ryouhei, Coatings of Nb-based alloy by Cr and/or Al pack cementations and its oxidation behavior in Air at 1273–1473 K, *Mater. Trans.*, 44(2003), No. 4, p. 731.

[33] C. Milanese, V. Buscaglia, F. Maglia, and U. Anselmi-Tamburini, Reactive growth of niobium silicides in bulk diffusion couples, *Acta Mater.*, 51(2003), No. 16, p. 4837.

[34] S. Prasad and A. Paul, Growth mechanism of phases by interdiffusion and diffusion of species in the niobium–silicon system, *Acta Mater.*, 59(2011), No. 4, p. 1577.

[35] M.A. Dayananda, An analysis of concentration profiles for fluxes, diffusion depths, and zero-flux planes in multicomponent diffusion, *Metall. Trans. A*, 14(1983), No. 9, p. 1851.

[36] P.C. Tortorici and M.A. Dayananda, Interdiffusion and diffusion structure development in selected refractory metal silicides, *Mater. Sci. Eng. A*, 261(1999), No. 1-2, p. 64.

[37] C.L. Yeh, H.J. Wang, and W.H. Chen, A comparative study on combustion synthesis of Ti–Si compounds, *J. Alloys Compd.*, 450(2008), No. 1-2, p. 200.